

FILIÈRE MÉTIERS DE LA RECHERCHE - SUJET 10

Radiological Pollution Monitoring: Anomaly Detection

Elisabeth LAHALLE

Ricardo CHIQUETTO DO LAGO
Maxsuel FERNANDES DE ALMEIDA
Samara NDIAYE
Ana Cecília REGHINI
Lucas TRAMONTE

September 2024

Contents

1	Introduction	2
2	Previous work	2
3	Methods	5
3.1	Global description	5
3.2	IQR method for training-data creation	5
3.3	Moving STD method	6
3.4	LSTM	6
3.4.1	Static Thresholding	7
3.4.2	Dynamic Thresholding	7
4	Results	8
4.1	IQR	8
4.2	STD	8
4.3	LSTM	9
5	Conclusion	11

1 Introduction

Gamma photons are often byproducts of radioactive decay processes, and their monitoring can be used as a way to detect and analyze radiation levels and ensure they stay within safe limits.

This work uses data collected in February, April, June and October 2015 for 28 days in each month. Measurements of gamma photons, atmospheric pressure, humidity and temperature were collected every minute during each of these periods.

Using this dataset, this study aims to select an unsupervised learning method, taking into account what is found in the literature and considering that the problem in hand involves time series.

2 Previous work

Monitoring anomalies in gamma radiation is essential for early detection of potential hazards, ensuring prompt action to safeguard public health and the environment. Therefore, it is critical to enhance detection systems to balance the need for sensitivity with minimizing false alarms. One example of its use was during the 2010 Winter Olympics. Sharma et al. (2012) [1] explore the use of machine learning algorithms for health-related radiological monitoring instead of gamma-ray spectrometers, that were used by the Canadian government and generated a significant number of false positives. The authors use the Mahalanobis distance (MD) as the anomaly detector, a method that works well for data with Gaussian distribution (a good approximation for the data of the authors), measuring how many standard deviations a data point is from the mean of the distribution. These distances are then ranked and the idea is that higher MD values are more likely to be anomalies. The authors conclude that further work should include an appropriate threshold, and that a limiting factor in Machine Learning is the scarcity of data of some classes.

Geiger-Müller tube (GMT) probes are one technique used by the European Radiological Exchange Platform (EURDEP) to centralize data from radiation monitoring networks for environmental gamma dose rate (GDR) monitoring. These inexpensive sensors have a limited spectrum information, which makes anomaly detection more difficult. Count rates are usually adjusted for background noise and temperature sensitivity in GDR measurements.

Environmental factors, particularly precipitation, pose challenges in radiation monitoring. Rain can transport radionuclides, causing spikes in dose rates, with variations in precipitation and other factors complicating accurate anomaly identification. Breitzkreutz et al. (2023) [2] investigate solutions to these issues. The study’s algorithm improves GDR anomaly detection through a series of steps:

- Data Augmentation: Combines GDR and weather data, flagging invalid entries.
- Precipitation Peak Removal: Uses a modified Livesay model to eliminate precipitation-induced GDR peaks.
- GDR Prediction: Employs an LSTM neural network to predict baseline GDR based on cleaned data.
- Anomaly Detection: Compares actual GDR with predicted baselines using Extreme Value Theory (EVT) and hierarchical clustering.

Although precipitation removal is effective, accuracy is decreased when local precipitation measurements are replaced by cloud reflectivity data. In terms of forecasting GDR baselines, Long

Short-Term Memory (LSTM) networks do well; aggregated data without autoregression or snow masking yields the best results. However, the DSPOT (Dynamic SPOT) algorithm frequently performs better than SPOT (Streaming Peaks Over Threshold), especially for short-term abnormalities, because of sporadic LSTM inaccuracies. Both these methods rely on the principle of Extreme Value Theory (EVT) to set the threshold and identify anomalies with the Peaks Over Threshold model, that relies on the on the Pickands-Balkema-de Haan theorem, which states that the values exceeding the threshold likely follow a generalized Pareto distribution. In SPOT, the threshold is adjusted so that it adapts to the changing distribution of the data, but it remains relatively stable during the detection process, while the DSPOT threshold is completely dynamic, not being so gradual as the SPOT. Rather than abrupt shifts, the SST (Statistical and Smoothed Trajectory features) method works better at detecting slow-evolving anomalies. This approach derives features from the time series and, by analyzing both statistical measures and the smoothed trajectory of the data, it creates a more comprehensive view of the series.

Poirier et al. (2022) [3] propose two new methods for detecting anomalies in gamma time series: a Matrix Profile-based method and a Crossmatch-based approach. Whereas the Crossmatch approach concentrates on finding similarities in time-series data, the Matrix Profile method lowers computing complexity. Both are compared to a standard moving standard deviation method, and while the Crossmatch approach suffers with noise but still works in other cases, the Matrix Profile method has short calculation time and performs well in noisy conditions. When motifs mimic background noise, the conventional technique is less successful even though it is fast and steady. These approaches demonstrate promise for real-time environmental monitoring when tested on simulated radiological data, and the article suggests that integrating them could improve signal monitoring systems. The limitation of this approach is the necessity of repetitive motifs to be identified, what can be a huge limitation.

One eminent application of unsupervised anomaly detection is in spacecraft systems, due to the particularities of space missions, such as its remote locations. Gao et al. (2012) [4] present an unsupervised method based on normal behavior clustering that employs large amounts of unlabelled telemetry data to construct a normal behavior model by identifying and eliminating abnormal data clusters. Subsequently, the model monitors real-time telemetry data, detecting any variations as possible anomalies. This approach is useful since it identifies unknown anomalies, as it does not rely on prior knowledge. The authors also discuss the limitations of traditional techniques that are too simplistic or heavily based on expert knowledge. In contexts where manual labeling and comprehensive knowledge modeling are difficult, the unsupervised technique offers a strong foundation for anomaly identification by clustering normal behavior and utilizing a nearest-neighbor algorithm to find outliers. The k-Nearest Neighbors (kNN) calculates the distance (weighted Euclidean distance) between a data point and its nearest neighbors. The distances to the k nearest neighbors are added resulting on the kNN score for that point. A small score indicates that the point is in a dense region of normal data, and a large score suggests that it is in a sparse region, likely being an anomaly.

According to Ergen et al. (2017) [5], one noteworthy strategy of unsupervised learning is the application of Long Short-Term Memory (LSTM) neural networks. This research presents algorithms based on LSTM for anomaly detection that are able to deal with variable-length data. The process consists in running sequences through an LSTM network to produce representations of fixed length, which are then used as inputs to Support Vector Data Description (SVDD) or One-Class Support Vector Machines (OC-SVM), and this joint use is achieved by gradient-based training techniques. This method allows the system to learn the best boundaries for anomaly detection and also the tem-

poral dependencies present in the data. Comparing this strategy against conventional procedures, there have been noticeable performance gains, especially when applied to time-series data.

Hundman et al. (2018) [6] also used LSTM for detecting anomalies in spacecraft systems, using the ability of it to model long time dependency and a groundbreaking method for setting dynamically the threshold above which a sequence is considered as anomalous. The authors give also a new way to mitigate the high number of false positives obtained with traditional methods, and explore the limits of traditional methods have been highlighted mostly in the case of collective and contextual anomalies.

The use of LSTM networks for anomaly detection is further explored by Malhotra et al. (2015) [7], who apply the technique to four real-world datasets: power demand, multi-sensor engine data, ECG signals, and Space Shuttle Marotta. Based on historical data, the model predicts future time steps, and anomalies are detected when the prediction error goes over a threshold. The error vectors are modelled to fit a multivariate Gaussian distribution, so the probability of these errors can be estimated. The results show that LSTM networks perform better than conventional recurrent neural networks (RNNs), particularly in situations where there are long-term dependencies. The authors find that stacked LSTM networks can accurately simulate the behavior of regular time series and identify abnormalities, which makes them appropriate for a range of anomaly detection applications.

Another way to address the anomaly detection task is to treat such problem as a change-point problem. Lavielle (2005) [8] explores this problem by proposing a statistical framework that leverages penalized contrasts functions of the type $J(\boldsymbol{\tau}, \mathbf{y}) + \beta \cdot \text{pen}(\boldsymbol{\tau})$ to estimate the number of change points and their locations in data sequences. In this framework, $J(\boldsymbol{\tau}, \mathbf{y})$ is the contrast function that measures the fit of the model $\boldsymbol{\tau}$, $\text{pen}(\boldsymbol{\tau})$ is a penalty term that depends on the dimension of the model and β is a penalization parameter that controls the balance between the fit and the penalty. The key contribution of this work is the introduction of an adaptive procedure to select the penalization parameter. The goal of this adaptive process is to determine the ideal penalization parameter value that yields a reliable and accurate estimate of the number of change points. The penalized contrast approach is highly suitable for anomaly detection in data, as anomalies often manifest as abrupt changes in the statistical properties of a sequence. By automatically determining the optimal number and location of change points, this method provides a powerful tool for identifying unexpected events in time series data, making it applicable to a wide range of anomaly detection tasks.

Kawahara and Sugiyama (2012) [9] address the change-point problem using the direct density-ratio estimation technique. The authors propose a non-parametric method that directly estimates the ratio of probability densities between reference and test intervals. This method is computationally efficient, suitable for online detection, and avoids the difficulties associated with density estimation. The approach is validated using both artificial and real-world datasets, demonstrating its flexibility and accuracy in detecting changes in various time-series scenarios.

Sinaga and Yang (2020) [10] propose a new algorithm, the U-k-means, an unsupervised clustering method that addresses the limitations of traditional k-means by eliminating the need for initialization and parameter selection. This method allows users to focus on analyzing the data without the burden of predefining the number of clusters, making U-k-means a robust choice for clustering tasks in diverse fields, with the proposition of a new objective function::

$$J_{U-k-means}(z, A, \alpha) = \sum_{i=1}^n \sum_{k=1}^c z_{ik} \|x_i - a_k\|^2 - \beta n \sum_{k=1}^c \alpha_k \ln \alpha_k - \gamma \sum_{i=1}^n \sum_{k=1}^c z_{ik} \ln \alpha_k$$

where $\|\mathbf{x}_i - \mathbf{a}_k\|$ is the Euclidean distance between the data point \mathbf{x}_i and the cluster center \mathbf{a}_k and z_{ik} is a binary variable indicating if the data point \mathbf{x}_i belongs to the k -th cluster.

3 Methods

3.1 Global description

The approach that has been chosen is to train a regression model on non-anomalous data to be able to accurately predict the next value x_{t+1} given a sequence x_1, x_2, \dots, x_t . The difference obtained between the errors of the regression model will be taken to decide where a new instance is anomalous or not. For the regression model, LSTM was naturally chosen for its ability to handle sequential data (as seen on [6] and [7]). As explained previously, LSTM are an extension of RNN that alleviate the explosion/evanescence problem and help to represent the long term dependency.

In order to train the LSTM model, a data set without anomalies is needed. In place of using visual criteria, this group decided to use two different statistical methods to estimate anomalies position and so prepare the data set. The IQR and the STD methods are those chosen. The dataset in reality is divided into 3 parts: a training set S_{train} , S_{val} and S_{test} . The last one is the only with anomalies inside.

Once the LSTM model was trained from the training data the errors from the testing set were obtained. Then, it is time to detect the anomalies from it. To achieve this objective, two approaches were tested in this project - static threshold and dynamic threshold. Python was used for all necessary programming.

3.2 IQR method for training-data creation

The first step was to select the data to be used to train the neural network. It was decided that the data from the first three months (February, April and June) would be used for training purposes, but they needed to be treated, as the training has to be done with measurements that are certainly not anomalous.

The first approach to identify the anomalies in the first three months was to use an algorithm implementing a statistical approach called "interquartile range", or IQR. The dataset is divided in quartiles. The first quartile (Q_1) is defined as the 25th percentile where lowest 25% data is below this point. The second quartile (Q_2) is the median of the dataset (50% of the data is below this point), and the third quartile (Q_3) is the 75th percentile where lowest 75% data is below this point. The IQR is defined by Eq. 1.

$$IQR = Q_3 - Q_1 \tag{1}$$

The outliers are then defined as the points that are below $Q_1 - 1.5 \cdot IQR$ or above $Q_3 + 1.5 \cdot IQR$.

However, this analysis is punctual, i.e. it does not allow the identification of "slow" anomalies, which is when a sequence of points shows a deviation. In order to be able to identify these anomalies,

another approach was implemented, based on the moving standard deviation (STD).

3.3 Moving STD method

The moving standard deviation method is based on that used as reference in [3]. It creates a threshold based on the moving mean (μ_m) and the moving standard deviation (σ_m) with windows those lengths are respectively $n \cdot lw$ and lw , where n is the multiplier for the moving mean's one that make it more stationary and create the comparison between a local STD and a "global" mean.

The next step is the determination of the threshold (th), given by Eq.2. This can be called as first threshold, as will be explained later, and so a first simple criterion for anomalies detection could be established just considering the points where the original signal passed this threshold.

$$th(t) = \mu_m(t) + 3 \cdot \sigma_m(t) \quad (2)$$

However, there are many points that overcame just a little and individually this first threshold that are mostly false positives. Then, to fix this sensibility, a moving mean was calculated from the *dif* signal obtained by the difference between the original signal ($x(t)$) and the first calculated threshold, as in Eq. 3. This ensures that big values of the *dif*'s mean will be obtained just when $dif(t) \approx 0$ (indicating a punctual anomaly) or when there are consecutive values of $dif(t) > 0$, indicating a collective anomaly.

$$dif(t) = \begin{cases} 0, & \text{if } x(t) \leq th(t) \\ x(t) - th(t), & \text{otherwise} \end{cases} \quad (3)$$

The next step is about establishing a minimal value of the moving mean of *dif*, above what an anomaly will be considered. That was done empirically and can be defined as a second threshold in the process, now static, to finally detect the motifs occurrences.

At the moment, the presence of motifs is detected, but not all their body. Usually, the center or the peak of the anomaly is detected, but the extremities of it did not pass the thresholds. So, in order to safely prepare the data set without any anomaly, a safety margin was included in motifs detection using **dilatation** operator. In addition, to avoid contaminated regions between close motifs, at the end, a **closing** operation was also used.

This method was, at the end, more effective than the IQR to the first anomalies' detection. So the dataset was prepared just using the conclusions from the moving STD method.

3.4 LSTM

The architecture that was selected contains two layers of LSTM with each 120 hidden units. Two dropout layers have been added between the LSTM in order to prevent overfitting which will cause the increase of false alarms. At the end of the model a dense layer was added with one unit and a linear activation. The model has been trained with the ADAM Optimizer and the Mean Squared Error is chosen as a loss function.

Layer (type)	Output Shape	Parameters
LSTM (120, activation ='relu')	(batch_size, 120)	58.560
Dropout (0.2)	(batch_size, 120)	0
LSTM (120, activation ='relu')	(batch_size, 120)	115.680
Dropout (0.2)	(batch_size, 120)	0
Dense (1, activation='linear')	(batch_size, 1)	121

Table 1: Model Architecture: 2 LSTM Layers, 2 Dropout Layers, 1 Dense Layer.

3.4.1 Static Thresholding

After the LSTM is trained, a set of errors e_{val} is obtained with S_{val} , and it is assumed that these errors follow a normal distribution

$$e_{val} \sim \mathcal{N}(\mu_{err}, \sigma_{e_{val}}^2).$$

with

$$\begin{aligned}\mu_{err} &= 1/N_{val} \sum e_{val} \\ \sigma_{err}^2 &= 1/N_{val} \sum (e_{val} - \mu_{err})^2\end{aligned}$$

Once a new instance x_{t+1} is given to the model, the LSTM uses the sequence x_1, x_2, \dots, x_t to predict \hat{y}_{t+1} and calculate the error $err = \hat{y}_{t+1} - x_{t+1}$, where

$$\begin{cases} x_{t+1} \text{ is normal if } \mathcal{N}(err) \leq \tau \\ x_{t+1} \text{ is anomalous, otherwise} \end{cases}$$

The threshold τ is set in order to have the best trade-off in term of precision and recall. It was found that the probability for the 99.5% quantile was a good value.

3.4.2 Dynamic Thresholding

The dynamic thresholding technique consists in dynamically selecting the threshold for different slices of the errors. To do so, first a window of errors $\mathbf{e} = [e^{(t-h)}, \dots, e^{(t-l_s)}, \dots, e^{(t-1)}, e^{(t)}]$ of length h is selected and smoothed using an exponentially-weighted average, leading to a sequence of smoothed errors $\mathbf{e}_s = [e_s^{(t-h)}, \dots, e_s^{(t-l_s)}, \dots, e_s^{(t-1)}, e_s^{(t)}]$. Then, for each window, it is selected as threshold the value ϵ from the set

$$\epsilon = \mu(\mathbf{e}_s) + z \cdot \sigma(\mathbf{e}_s),$$

that maximizes the Equation 4.

$$\frac{\frac{\Delta\mu(\mathbf{e}_s)}{\mu(\mathbf{e}_s)} + \frac{\Delta\sigma(\mathbf{e}_s)}{\sigma(\mathbf{e}_s)}}{|e_a| + |\mathbf{E}_{seq}|^2}, \quad (4)$$

where:

$$\begin{aligned}
z &= [2.0, 2.5, \dots, 9.5, 10.0] \\
\Delta\mu(\mathbf{e}_s) &= \mu(\mathbf{e}_s) - \mu(\{e_s \in \mathbf{e}_s | e_s < \epsilon\}) \\
\Delta\sigma(\mathbf{e}_s) &= \sigma(\mathbf{e}_s) - \sigma(\{e_s \in \mathbf{e}_s | e_s < \epsilon\}) \\
\mathbf{e}_a &= \{e_s \in \mathbf{e}_s | e_s > \epsilon\} \\
\mathbf{E}_{seq} &: \text{continuous sequences of } e_a \in \mathbf{e}_a
\end{aligned}$$

The idea behind this procedure is, for each window, to select as threshold the value ϵ so that if all the values above it are removed, the percentage decrease in the mean and the standard deviation of the smoothed errors \mathbf{e}_s are maximized, while penalizing for having large number of anomalous values ($|\mathbf{e}_a|$) and continuous anomalous sequences ($|\mathbf{E}_{seq}|$). The advantages of such method lie in the fact that it does not rely in the use of a big set of labeled data or in statistical assumptions about the errors.

For the implementation, the code provided by [6] was adapted to the current problem.

4 Results

4.1 IQR

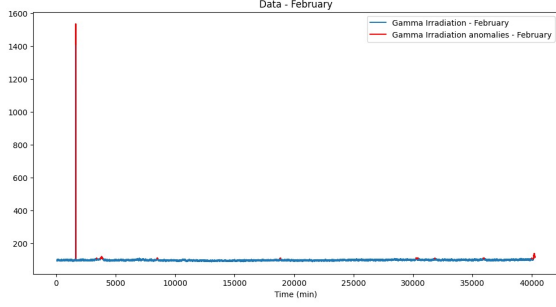
Regarding the IQR, the results obtained for the three months are shown in Fig. 1. There are two plots for February because the data acquired had a very noticeable peak in the beginning, close to $t = 2500 \text{ min}$, that had a value close to 1500 (Fig. 1a). As the remaining values were all very below this value (all below 150), it was concluded that said peak was a sensor error, thus being removed (Fig. 1b).

4.2 STD

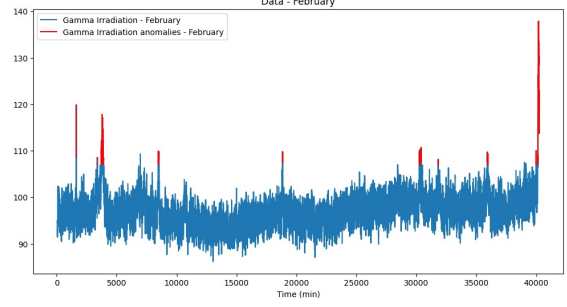
For the moving STD, the detected motifs (anomalous patterns) are presented in Fig. 2. The parameters chosen to obtain this results were: $lw = 20$, $n = 70$ and minimal dif 's mean to detect motifs as 0.3 . In observation, the second graph is multiplied by a factor of 10 in the figure, so the threshold is represented as 3.

Visually, the method could well transmit with the dif 's mean (second graph) the chance of motif's existence. As an unlabeled problem, it is difficult to establish a more exact performance index.

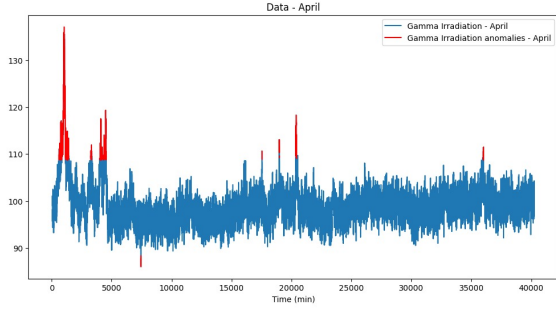
For the test set (October), the detected motifs (anomalous patterns) of the LSTM and STD methods are presented in Fig. 3 and 4 .



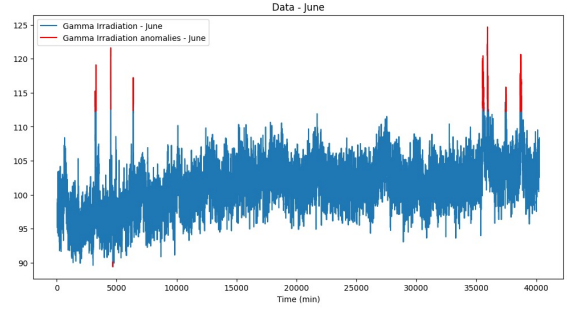
(a) IQR outliers - February



(b) IQR outliers - February (corrected)



(c) IQR outliers - April



(d) IQR outliers - June

Figure 1: Outliers found with the IQR

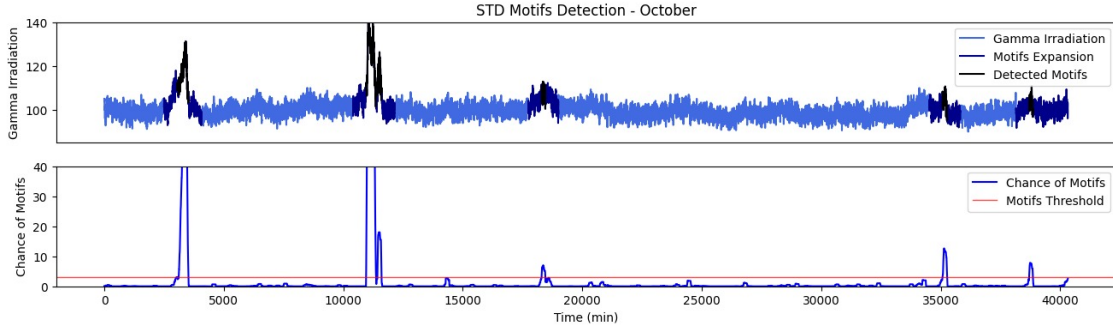
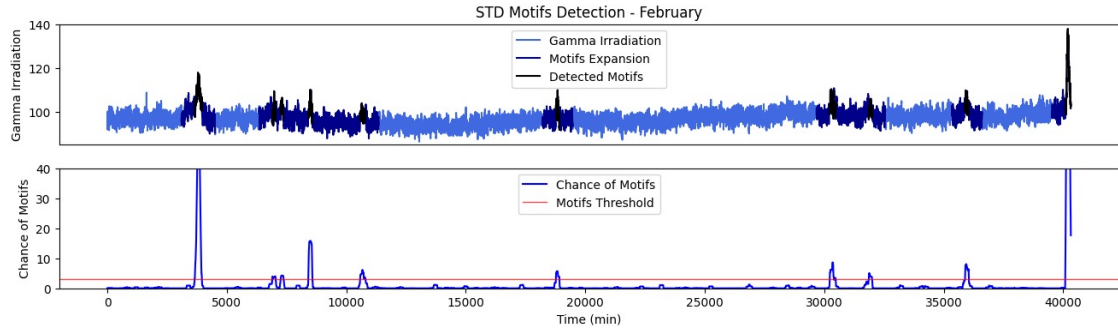


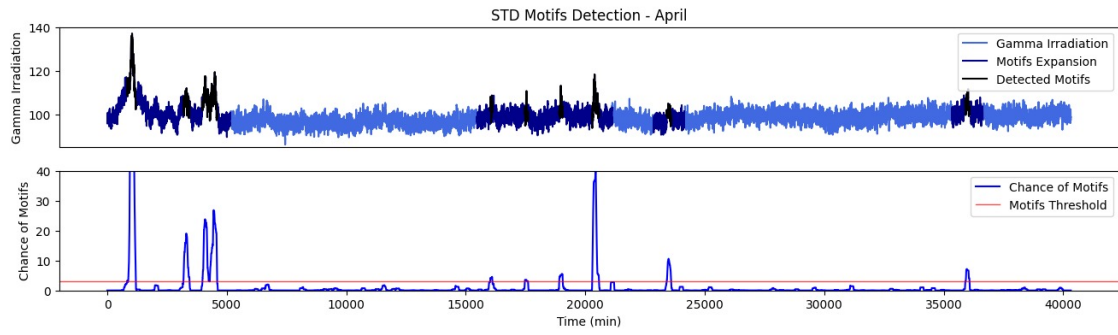
Figure 3: October motifs detected with moving STD method.

4.3 LSTM

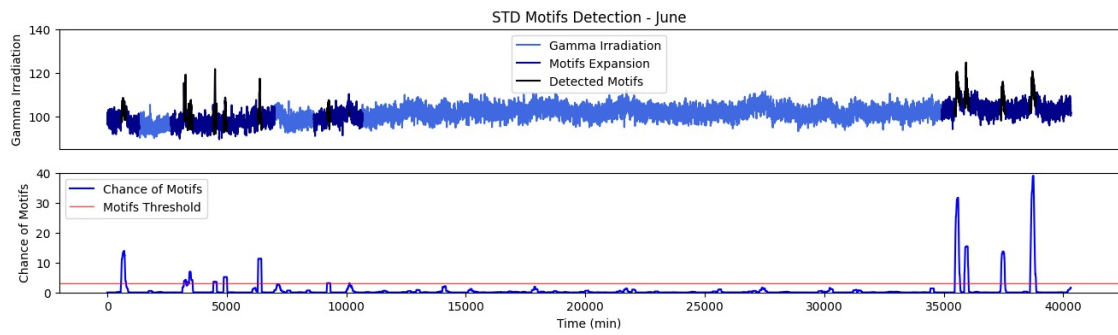
Figure 4 presents the result of the LSTM implemented with a static threshold. The pink line (bottom plot) indicates the probability of the corresponding part on the top plot of being an anomaly. It is noticeable that most of the anomalous motifs have been detected by the model but with some false positives. It was observed during development that for this method that the results improve when the number of units in the LSTM and the training data is increased. Additional work needs to be done for a better tuning of the parameters.



(a) February motifs



(b) April motifs



(c) June motifs

Figure 2: Detected motifs with the moving STD method

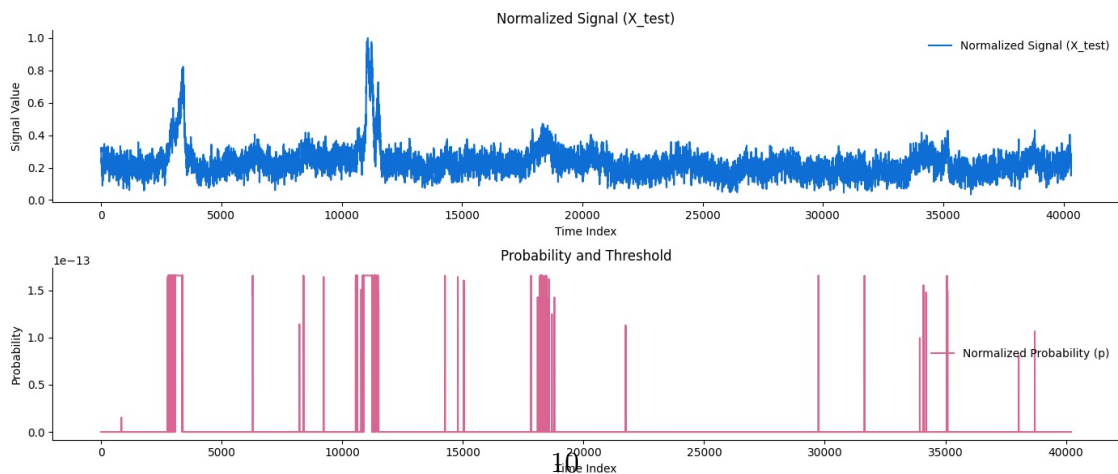


Figure 4: October motifs detected with LSTM with static threshold.

The result obtained by the LSTM implemented with dynamic threshold is presented in Figure 5. In this figure, the anomalous motifs detected by the method are marked in dark blue.

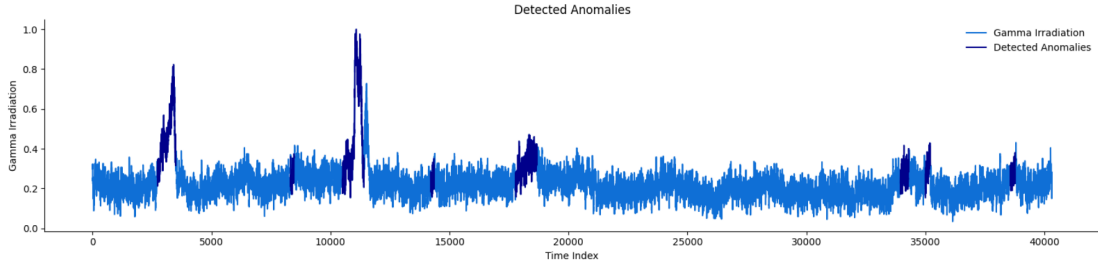


Figure 5: October motifs detected with LSTM with dynamic threshold.

The presented result shows that the dynamic threshold method is capable of predict the anomalies with less false positives than the static one, with the advantage of not doing assumptions about statistical properties of the errors. A better performance can be achieved with the correct tuning of hyper-parameters like the amount of historical error (h) used to evaluate new errors and the batch size used in the evaluation.

5 Conclusion

Considering the limited time for implementation, the LSTM presented good results, slightly more precise than the one given by the moving STD method. One possible way to refine more the results is to make separate measures of the gamma photons in normal atmospheric conditions and during rain, for it transports radionuclides, causing spikes in dose rates and affecting anomaly detection, as discussed before.

Regarding the dynamic thresholding, the results obtained were not as detailed as the results obtained with the static threshold. The detections were mostly only the peaks of the signal, not detecting the slow anomalies. This could be improved during a longer development time.

References

- [1] Shiven Sharma, Colin Bellinger, Nathalie Japkowicz, Rodney Berg, and Kurt Ungar. Anomaly detection in gamma ray spectra: A machine learning perspective. In *2012 IEEE Symposium on Computational Intelligence for Security and Defence Applications*, pages 1–8, 2012.
- [2] Harald Breitzkreutz, Josef Mayr, Martin Bleher, Stefan Seifert, and Ulrich Stöhlker. Identification and quantification of anomalies in environmental gamma dose rate time series using artificial intelligence. *Journal of Environmental Radioactivity*, 259-260:107082, 2023.
- [3] Lisa Poirier-Herbeck, Elisabeth Lahalle, Nicolas Saurel, and Sylvie Marcos. Unknown-length motif discovery methods in environmental monitoring time series. In *2022 International Conference on Electrical, Computer and Energy Technologies (ICECET)*, pages 1–5, Prague, Czech Republic, 2022.
- [4] Yu Gao, Tianshe Yang, Minqiang Xu, and Nan Xing. An unsupervised anomaly detection approach for spacecraft based on normal behavior clustering. In *2012 Fifth International Conference on Intelligent Computation Technology and Automation*, pages 478–481. IEEE, 2012.
- [5] Tolga Ergen, Ali H. Mirza, and Suleyman S. Kozat. Unsupervised and semi-supervised anomaly detection with lstm neural networks. *arXiv preprint arXiv:1710.09207*, 2017.
- [6] Kyle Hundman, Valentino Constantinou, Christopher Laporte, Ian Colwell, and Tom Soderstrom. Detecting spacecraft anomalies using lstms and nonparametric dynamic thresholding. In *Proceedings of the 24th ACM SIGKDD International Conference on Knowledge Discovery & Data Mining*, KDD ’18, page 387–395, New York, NY, USA, 2018. Association for Computing Machinery.
- [7] Pankaj Malhotra, Lovekesh Vig, Gautam M. Shroff, and Puneet Agarwal. Long short term memory networks for anomaly detection in time series. In *The European Symposium on Artificial Neural Networks*, 2015.
- [8] Marc Lavielle. Using penalized contrasts for the change-point problem. *Signal Processing*, 85(8):1501–1510, 2005.
- [9] Yoshinobu Kawahara and Masashi Sugiyama. Sequential change-point detection based on direct density-ratio estimation. *Statistical Analysis and Data Mining*, 5(2):114–127, 2012.
- [10] Kristina P. Sinaga and Miin-Shen Yang. Unsupervised k-means clustering algorithm. *IEEE Access*, 8:80716–80727, 2020.